RSC Advances

PAPER

View Article Online
View Journal | View Issue

Cite this: *RSC Adv.*, 2019, **9**, 29429

A formation model of superoxide radicals photogenerated in nano-TiO_2 suspensions†

Dabin Wang,[a] Lixia Zhao,*[b] Dean Song,[a] Jun Qiu,[a] Fanyu Kong*[a] and Liang-Hong Guo[b]

Received 14th August 2019
Accepted 23rd August 2019

DOI: 10.1039/c9ra06323d

rsc.li/rsc-advances

A formation model of $O_2^{\cdot-}$ produced in TiO_2 photocatalysis was established, and then a custom built continuous flow chemiluminescence (CFCL) system was used to confirm the model's reliability by monitoring the $O_2^{\cdot-}$ formation process. This model may give deeper insights into $O_2^{\cdot-}$ formation for TiO_2 and other photocatalysts.

In photocatalytic reactions, such as TiO_2, it is generally accepted that $O_2^{\cdot-}$ is produced from the reduction of adsorbed oxygen by photogenerated electrons on the TiO_2 surface.[1–5] $O_2^{\cdot-}$ formation is a rate-limiting process in TiO_2 photocatalytic reactions,[6] and thus determines the efficiency of TiO_2 photocatalytic reactions by promoting the separation of photogenerated electrons and holes. Moreover, $O_2^{\cdot-}$ is an intriguing active species, attracting a great deal of attention in recent years due to its unique role. Previous studies have confirmed that $O_2^{\cdot-}$ plays an essential role in the photodegradation of pollutants.[7,8] Therefore, probing the dynamic formation of $O_2^{\cdot-}$ over the course of time under UV irradiation is conducive to better understanding TiO_2 photocatalytic reactions. We have successfully identified surface long-lived $O_2^{\cdot-}$ photogenerated on TiO_2 surface,[9] however, the dynamic details of $O_2^{\cdot-}$ formation in TiO_2 photocatalytic reactions still remain to be solved.

In photocatalytic reactions, $O_2^{\cdot-}$ is continuously undergoing the processes of formation and deactivation simultaneously. Many methods have been developed to determine the $O_2^{\cdot-}$, including electron spin resonance (ESR),[10] spectrophotometric assays,[11–13] and fluorescence assays,[14,15] but the $O_2^{\cdot-}$ could only be detected at discrete times, and thus the total quantity could only be given within the irradiation duration. Given these limitations, $O_2^{\cdot-}$ dynamic monitoring is a great challenge. Chemiluminescence (CL) is inherently sensitive and rapid due to the relative ease with which light emission is instantly generated through a chemical reaction when two or more reactants are mixed. These qualities of CL make it suitable for the dynamic study of $O_2^{\cdot-}$, despite its characteristic instability. In a previous study, we were able to successfully develop a continuous flow chemiluminescence (CFCL) method for dynamic monitoring of the formation process of $O_2^{\cdot-}$ in TiO_2 photocatalytic reactions.[16]

For the formation mechanism of $O_2^{\cdot-}$ in TiO_2 photocatalytic reactions, it is generally accepted that $O_2^{\cdot-}$ formation occurs on TiO_2 surfaces by the following scheme:

$$O_2 + S \underset{k_{-1}}{\overset{k_1}{\rightleftharpoons}} O_{2,s} \xrightarrow{k_f} O_{2,s}^{\cdot-} \xrightarrow{k_d} O_2, H_2O_2$$

where O_2 denotes the dissolved oxygen (DO) in solution, S denotes the oxygen adsorption site on TiO_2 surface, k_1 and k_{-1} denote the adsorption/desorption rate constant of O_2 respectively, $O_{2,s}$ denotes the adsorbed oxygen on TiO_2 surface, k_f denotes the formation rate constant of $O_2^{\cdot-}$, $O_{2,s}^{\cdot-}$ denotes the $O_2^{\cdot-}$ formed on TiO_2 surface, and k_d denotes the rate constant of $O_2^{\cdot-}$ decomposition. It was reported that DO was first adsorbed on the site of TiO_2 surface following the Langmuir isotherm,[6] and then the adsorbed O_2 was reduced to $O_2^{\cdot-}$ by photogenerated electrons under UV irradiation. Meanwhile, the formed $O_2^{\cdot-}$ was transformed into other species by side reactions, such as H_2O_2 or $^1O_2$ which deactivated to O_2 quickly. Specifically, it is suggested by some research that $O_2^{\cdot-}$ could be produced from the oxidation of H_2O_2 by valence-band hole (h^+) or hydroxyl radical ($\cdot OH$) in solution, where H_2O_2 is produced by the two-step oxidation of water or the two-electron reduction of O_2.[17] It is insignificant in this study because the $O_2^{\cdot-}$ detected by CFCL method is the long-lived superoxide adsorbed on TiO_2 surface which is produced from the reduction of O_2 by photogenerated electrons, not in solution according to our previous study.[9] The process of $O_2^{\cdot-}$ formation was illustrated concretely as follows: when TiO_2 semiconductor is irradiated, the photogenerated electrons transferring to the TiO_2 surface are captured by five-coordinated surface Ti^{4+} to form the Ti^{3+} (eqn

[a]*Laboratory of Quality & Safety Risk Assessment for Tobacco, Ministry of Agriculture, Tobacco Research Institute of Chinese Academy of Agricultural Sciences, Qingdao 266101, China. E-mail: kongfanyu@caas.cn; Fax: +86-532-88703386; Tel: +86-532-88703386*

[b]*State Key Laboratory of Environmental Chemistry and Ecotoxicology, Research Center for Eco-Environmental Sciences, Chinese Academy of Sciences, P. O. Box 2871, 18 Shuangqing Road, Beijing 100085, China. E-mail: zlx@rcees.ac.cn; Fax: +86-10-62849685; Tel: +86-10-62849338*

† Electronic supplementary information (ESI) available. See DOI: 10.1039/c9ra06323d

(1)). Then the O_2 adsorbed on TiO_2 surface react with Ti^{3+} to form $O_2^{\bullet-}$ (eqn (2)).[1,2,18]

$$-Ti^{4+}-OH + e \rightarrow -Ti^{3+} + OH^- \quad (1)$$

$$-Ti^{3+} + O_{2,s} \rightarrow -Ti^{4+}\cdots OO^{\bullet-} \quad (2)$$

$$O_2^{\bullet-} + h^+/\cdot OH \rightarrow {}^1O_2 \quad (3)$$

$$O_2^{\bullet-} + e + H^+ \rightarrow H_2O_2 \quad (4)$$

$$O_2^{\bullet-} + O_2^{\bullet-} + H^+ \rightarrow H_2O_2 + O_2 \quad (5)$$

Meanwhile, $O_2^{\bullet-}$ formed also undergoes a decaying process possibly *via* the following three pathways (eqn (3)–(5)): (1) oxidation by h^+ or $\cdot OH$, (2) further reduction by e, or (3) self-disproportionation in solution. Therefore, the number of $O_2^{\bullet-}$ determined in photocatalytic reactions at any irradiation time (t) is what the total quantity of formed $O_2^{\bullet-}$ subtract those decomposed *via* the aforementioned side reactions from t_0 s to t s upon irradiation. The formula can be expressed as follows:

$$\left[O_2^{\bullet-}\right]_t = \int_{t_0}^{t} \mathrm{d}\left[O_2^{\bullet-}\right]_f \Big/ \mathrm{d}t - \int_{t_0}^{t} \mathrm{d}\left[O_2^{\bullet-}\right]_d \Big/ \mathrm{d}t \quad (6)$$

In this equation, the t_0 and t of the lower and upper limit of the definite integral represent the starting and ending time of UV irradiation respectively. Based on the formation process of $O_2^{\bullet-}$ mentioned above, the net rate of $O_2^{\bullet-}$ formation at any time in photocatalytic reactions can be obtained as shown in eqn (7.1). The first term of the right side of the eqn (7.1) represents the formation rate of $O_2^{\bullet-}$, and it is a second-order reaction with respect to the concentration of $-Ti^{3+}$($[Ti^{3+}]$) and adsorbed oxygen ($O_{2,s}$). k_f is a second-order formation rate constant. The second term (eqn (7.1)) represents the decay rate of $O_2^{\bullet-}$, among which k_d is a second-order decay rate constant, [X] represents the concentration of e, h^+, $\cdot OH$ or $O_2^{\bullet-}$ in terms of eqn (3)–(5). It is generally believed to contain the aforementioned three pathways. We have previously confirmed that the $O_2^{\bullet-}$ adsorbed on TiO_2 surface is thermodynamically favored.[9] Therefore, the two former pathways (eqn (3) and (4)) dominated the decay process under UV irradiation. These processes were considered to be pseudo-first-order due to the constant of h^+, $\cdot OH$ and e under steady-state irradiation. So k'_d($k'_d = k_d \times [X]$) is the pseudo-first-order apparent rate constant (eqn (7.2)). $[O_2]_s$ is equal to oxygen coverage on TiO_2 surface (θ) by the number of adsorption sites ([S]) according to Langmuir isotherm (eqn (7.2)), in which θ is related to the DO concentration in solution ($[O_2]$), adsorption constant (k_1), desorption constant (k_{-1}), and formation rate constant of $O_2^{\bullet-}$ (k_f) (eqn (7.3)).

$$\frac{\mathrm{d}\left[O_2^{\bullet-}\right]}{\mathrm{d}t} = k_f\left[Ti^{3+}\right][O_2]_s - k_d[X]\left[O_2^{\bullet-}\right] \quad (7.1)$$

$$= k_f\left[Ti^{3+}\right]\theta[S] - k'_d\left[O_2^{\bullet-}\right] \quad (7.2)$$

$$= k_f\left[Ti^{3+}\right][S]\frac{k_1[O_2]}{k_1[O_2] + k_{-1} + k_f} - k'_d\left[O_2^{\bullet-}\right] \quad (7.3)$$

It has been reported that the electron transfer from TiO_2 to O_2 is the rate-limiting step in TiO_2 photocatalytic reaction.[6,19–21] Upon this, k_f is far less than $k_1[O_2]$ and k_{-1}. Furthermore, the $[O_2]$ in solution is low, and thus $k_1[O_2]$ is far less than k_{-1}. If such speculation is true, the eqn (7.3) can be eventually transformed into the following:

$$\frac{\mathrm{d}\left[O_2^{\bullet-}\right]}{\mathrm{d}t} = k_f\left[Ti^{3+}\right][S]K_1[O_2] - k'_d\left[O_2^{\bullet-}\right] \quad (8)$$

where K_1 ($K_1 = k_1/k_{-1}$) is the adsorption equilibrium constant of $[O_2]$. Assuming that $[O_2^{\bullet-}] = m\mathrm{CL} + n$, which is a linear relationship between $O_2^{\bullet-}$ concentration and CL intensity, the eqn (8) can then be converted into the following:

$$\frac{\mathrm{d}[m\mathrm{CL} + n]}{\mathrm{d}t} = k_f\left[Ti^{3+}\right][S]K_1[O_2] - k'_d[m\mathrm{CL} + n] \quad (9)$$

Finally, the eqn (10) representing the formation model of $O_2^{\bullet-}$, with respect to time as the independent variable and CL intensity as the dependent variable, would be obtained by integrating these variables with the eqn (9) from t_0 to t:

$$\mathrm{CL} = \frac{k_f K_1[Ti^{3+}][S][O_2]}{mk'_d}\left(1 - e^{-k'_d(t-t_0)}\right) + \frac{n}{m} \quad (10)$$

In eqn (10), k_f, K_1, k'_d, [S], $[O_2]$, m, and n are constants under certain conditions. The coefficient $((k_f K_1[Ti^{3+}][S][O_2]/(mk'_d)) + n/m)$ represents the theoretical maximum CL intensity (CL_0) corresponding to the steady-state concentration of $O_2^{\bullet-}$ when t is infinite in irradiated TiO_2 suspensions. Herein t_0 is the time when irradiation starts for 50 s, due to the disturbance of background signal within the first 50 s of irradiation. According to eqn (10), given that k_f, K_1, and k_d are determined by the intrinsic property of TiO_2 photocatalyst regardless of experimental conditions, CL_0 is dependent on $[Ti^{3+}]$, [S], $[O_2]$ and [X], which are closely related to experimental conditions. In photocatalytic reactions, $[Ti^{3+}]$ relies on the number of photogenerated electrons highly dependent on I; [S] is the total surface area of TiO_2 in suspension, closely related to $[TiO_2]$; $[O_2]$ is dependent on [DO] in TiO_2 suspensions; [X], the aforementioned concentration of h^+, $\cdot OH$ and e, is also dependent on I.

In order to verify the formation model of $O_2^{\bullet-}$, we fit the different CL curves with eqn (10) by changing $[TiO_2]$, I, and [DO]. As shown in Fig. 1(a–i), the CL curves from different $[TiO_2]$, I and [DO] were well-fit by eqn (10) with high correlation coefficients ($R^2 > 0.99$), indicating that the model could simulate dynamic process of $O_2^{\bullet-}$ formation. Furthermore, according to the $O_2^{\bullet-}$ formation model (eqn (10)), CL intensity is linearly correlated to [S], $[Ti^{3+}]$, and $[O_2]$, indicating that CL intensity could increase linearly with the increase of $[TiO_2]$, I and [DO] within set limits. In order to verify this assumption, CL intensity at 300 s, 600 s, 900 s, 1200 s and $+\infty$ under different $[TiO_2]$, I and [DO] conditions in TiO_2 suspensions was calculated by eqn (10) (Table S1†). Then the CL intensity from different $[TiO_2]$, I and [DO] at different time points were linearly fit (Fig. S1–

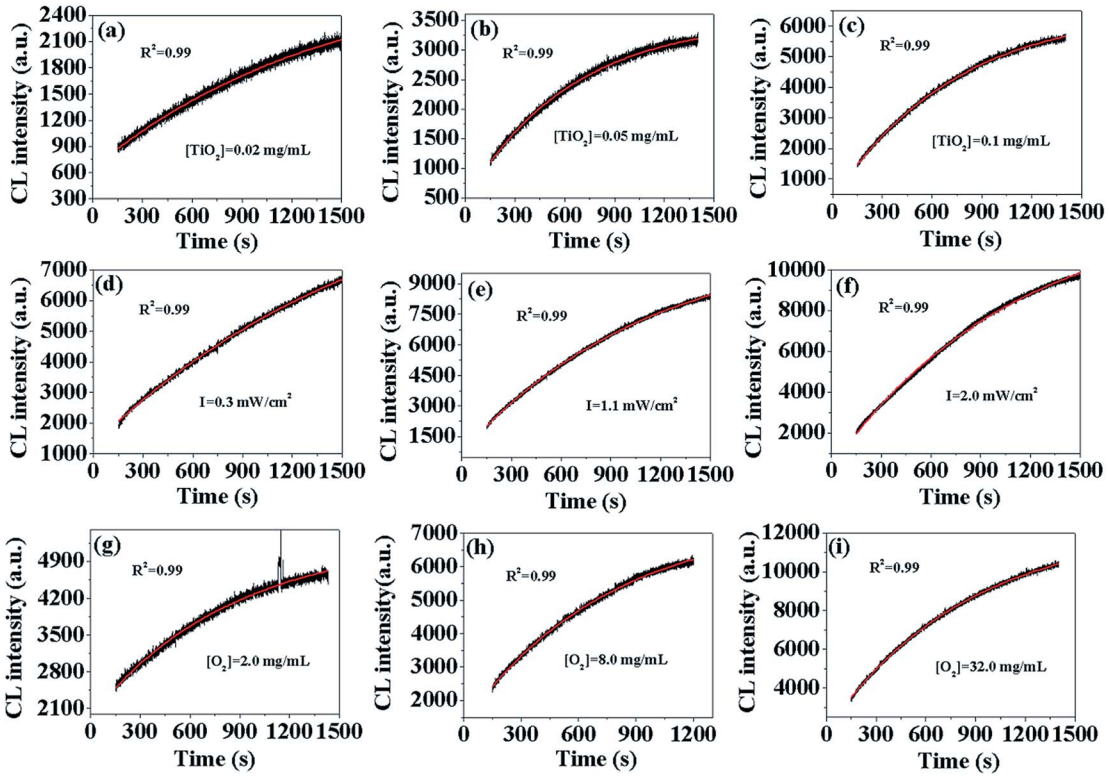

Fig. 1 CL curves of luminol (50 μM) with photo-irradiated TiO_2 suspensions (pH = 11) under different experimental conditions: TiO_2 concentration (a–c), irradiation intensity (d–f), DO concentration (g–i). The black lines represent experimentally measured values and the red lines are the fitted values.

3†), and the R square values were calculated and summarized in Table 1. For instance, the CL intensity with TiO_2 concentration of 0.02 mg mL^{-1}, 0.05 mg mL^{-1} and 0.1 mg mL^{-1} at 300 s, 600 s, 900 s, 1200 s and $+\infty$, respectively, had good linear fit with high correlation coefficients ($R^2 > 0.99$), except at $+\infty$ ($R^2 = 0.903$), confirming that CL intensity increased linearly with the increase of [S] as indicated by eqn (10). There was also a good linear relationship between CL intensity and I with high correlation coefficients ($R^2 > 0.9$), except at $+\infty$ ($R^2 = 0.821$), indicating that CL intensity increased linearly with the increase of $[Ti^{3+}]$. At different [DO], the corresponding R^2 values were also high ($R^2 > 0.95$), indicating that CL intensity was also linearly dependent on $[O_2]$. Overall, the formation model of $O_2^{\bullet-}$ could adequately describe the dynamic process of $O_2^{\bullet-}$ formation in photo-irradiated TiO_2 suspensions.

In the present work, a formation model of $O_2^{\bullet-}$ in TiO_2 photocatalytic reactions was established. According to the model, the $O_2^{\bullet-}$ formation was closely related with $[TiO_2]$, [DO] and I, under which the dynamic process of $O_2^{\bullet-}$ formation was successfully simulated by the model with high correlation coefficients ($R^2 > 0.9$), thereby confirming the model validity. This model can explicitly provide details on $O_2^{\bullet-}$ formation which determines the photocatalytic efficiency in TiO_2 photocatalytic reactions, and give deeper insights into designing high-efficiency TiO_2 photocatalysts. In accordance with this model, Feng *et al.* reported the self-doped Ti^{3+} enhanced TiO_2 photocatalyst for hydrogen production through the reduction of the TiO_2 surface using a one-step combustion method.[22] Furthermore, this model may have significant implications for other photocatalysts with respect to $O_2^{\bullet-}$ formation.

Table 1 The calculated value of R square upon different experimental conditions at different irradiation time

Time (s)	TiO_2 concentration (mg mL^{-1})	Irradiation intensity (mW cm^{-2})	DO concentration (mg mL^{-1})
300	0.998	0.921	0.999
600	0.999	0.946	0.982
900	0.998	0.960	0.971
1200	0.994	0.972	0.968
$+\infty$	0.903	0.821	0.977

Conflicts of interest

There are no conflicts to declare.

Acknowledgements

The authors gratefully acknowledge financial support from the Agricultural Science and Technology Innovation Program (ASTIP-TRIC06), National Key Research and Development Program of China (2016YFA0203102), National Natural Science Foundation of China (31601483, 31801646, 21876184, 21677152), Fundamental Research Funds for Central Non-profit Scientific Institution (1610232017011, 1610232016008, 1610232017010, 1610232018002).

Notes and references

1 Y. Nakaoka and Y. Nosaka, *J. Photochem. Photobiol., A*, 1997, **110**, 299–305.
2 A. L. Attwood, D. M. Murphy, J. L. Edwards, T. A. Egerton and R. W. Harrion, *Res. Chem. Intermed.*, 2003, **29**, 449–465.
3 M. A. Henderson, W. S. Epling, C. H. F. Peden and C. L. Perkins, *J. Phys. Chem. B*, 2003, **107**, 534–545.
4 E. Carter, A. F. Carley and D. M. Murphy, *J. Phys. Chem. C*, 2007, **111**, 10630–10638.
5 J. Green, E. Carter and D. M. Murphy, *Chem. Phys. Lett.*, 2009, **477**, 340–344.
6 M. R. Hoffmann, S. T. Martin, W. Choi and D. W. Bahnemann, *Chem. Rev.*, 1995, **95**, 69–96.
7 C. Chen, P. Lei, H. Ji, W. Ma and J. Zhao, *Environ. Sci. Technol.*, 2004, **38**, 329–337.
8 J. Yang, C. C. Chen, H. W. Ji, W. H. Ma and J. C. Zhao, *J. Phys. Chem. B*, 2005, **109**, 21900–21907.
9 D. Wang, L. Zhao, D. Wang, L. Yan, C. Jing, H. Zhang, L.-H. Guo and N. Tang, *Phys. Chem. Chem. Phys.*, 2018, **20**, 18978–18985.
10 J. Sun, H. Zhang, L.-H. Guo and L. Zhao, *ACS Appl. Mater. Interfaces*, 2013, **5**, 13035–13041.
11 M. W. Sutherland and B. A. Learmonth, *Free Radical Res.*, 1997, **27**, 283–289.
12 B. H. J. Blelski, G. G. Shiue and S. Bajuk, *J. Phys. Chem.*, 1980, **84**, 830–833.
13 Y. Li, W. Zhang, J. Niu and Y. Chen, *ACS Nano*, 2012, **6**, 5164–5173.
14 S. T. Wang, N. G. Zhegalova, T. P. Gustafson, A. Zhou, J. Sher, S. Achilefu, O. Y. Berezin and M. Y. Berezin, *Analyst*, 2013, **138**, 4363–4369.
15 K.-I. Ishibashi, A. Fujishima, T. Watanabe, K. Hashimoto, K. Ishibashi, A. Fujishima and T. Watanabe, *J. Photochem. Photobiol., A*, 2000, **134**, 139–142.
16 D. Wang, L. Zhao, L. H. Guo and H. Zhang, *Anal. Chem.*, 2014, **86**, 10535–10539.
17 Y. Nosaka and A. Y. Nosaka, *Chem. Rev.*, 2017, **117**, 11302–11336.
18 T. Daimon, T. Hirakawa, M. Kiazawa, J. Suetake and Y. Nosaka, *Appl. Catal., A*, 2008, **340**, 169–175.
19 C. M. Wang, A. Heller and H. Gerischer, *J. Am. Chem. Soc.*, 1992, **114**, 5230–5234.
20 H. Gerischer and A. Heller, *J. Electrochem. Soc.*, 1992, **139**, 113–118.
21 A. M. Peiró, C. Colombo, G. Doyle, J. Nelson, A. Mills and J. R. Durrant, *J. Phys. Chem. B*, 2006, **110**, 23255–23263.
22 F. Zuo, L. Wang, T. Wu, Z. Zhang, D. Borchardt and P. Feng, *J. Am. Chem. Soc.*, 2010, **132**, 11856–11857.